Supporting Information for

High-Temperature Anomalous Hall Effect in Transition Metal Dichalcogenide-Ferromagnetic Insulator Heterostructure

Sheung Mei Ng[1†], Huichao Wang[1,2†], Yukuai Liu[1], Hon Fai Wong[1], Hei Man Yau[1], Chun Hung Suen[1], Ze Han Wu[1], Chi Wah Leung[1] and Ji-Yan Dai[1*]

[1]*Department of Applied Physics, The Hong Kong Polytechnic University, Hong Kong, 999077, P. R. China*

[2]*School of Physics, Sun Yat-Sen University, Guangzhou 510275, China*

[*]E-mail: jiyan.dai@polyu.edu.hk

‡ S.M.N. and H.C.W. contributed equally.

Figure S1. EDX spectrum from different layers. In the amorphous layer, the presence of Y and Fe suggests the composition related to YIG (O is not shown) while the presence of Te suggests the diffusion from $ZrTe_2$ (Gd is from substrate GGG). The EDX result suggests the layer is amorphous YIG with Te.

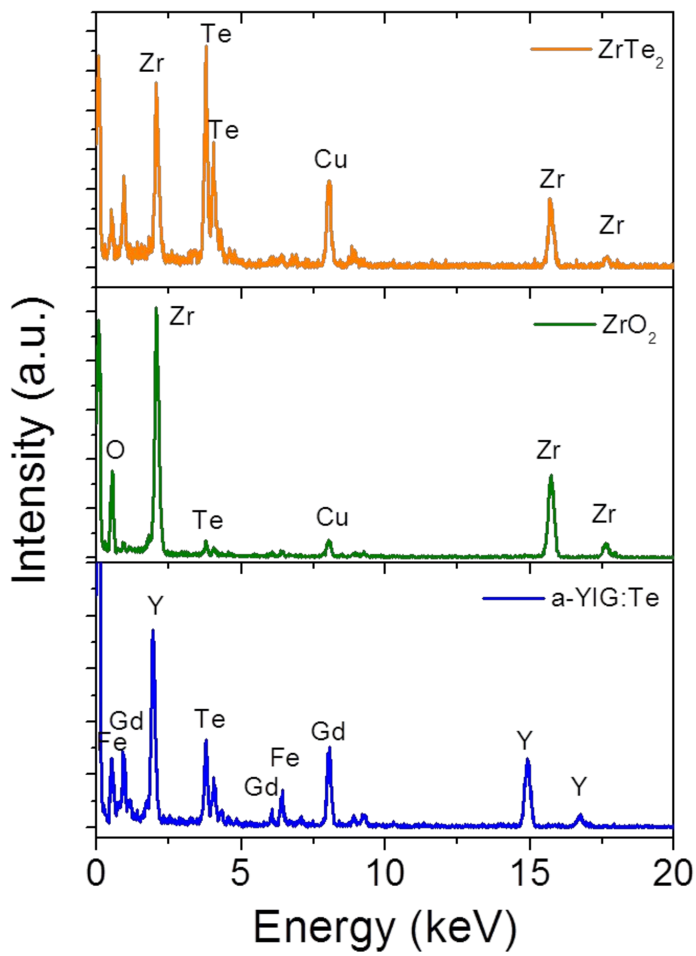

Figure S2. TEM image of sample with a short deposition time and ZrO_2 and a-YIG:Te were formed but not yet layered $ZrTe_2$, and such structure shows high resistance (>20MΩ), suggesting ZrO_2 and a-YIG:Te layers are insulating.

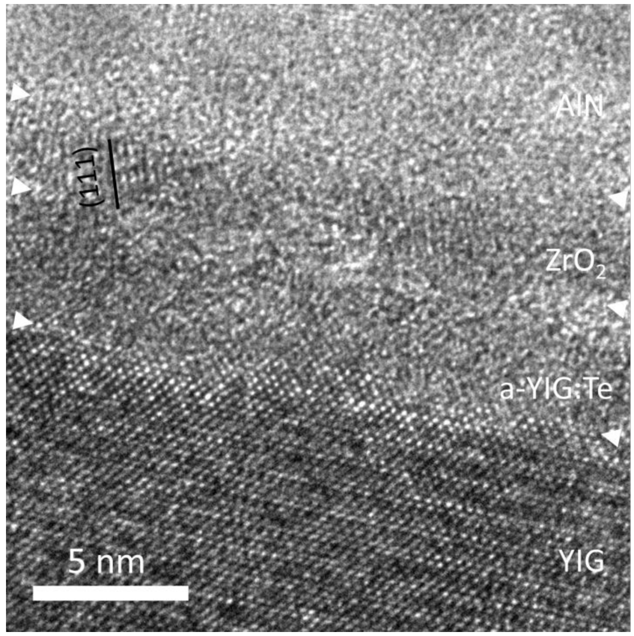

Figure S3. The anomalous Hall effect (R_{AHE}) was obtained by subtracting the linear background, which is contribution of ordinary Hall effect as indicated by the red dashed line in (a), from the total Hall resistance (R_{yx}).

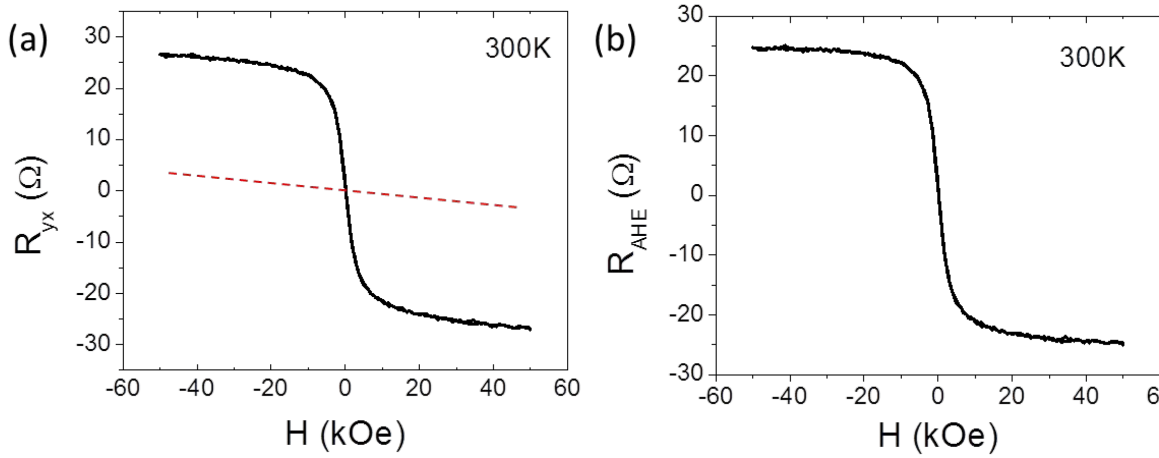

Figure S4. The anomalous Hall effect (R_{AHE}) at selected temperatures for the 18 nm thick $ZrTe_2$ thin film within the heterostructure. The curves are shifted for clarity.

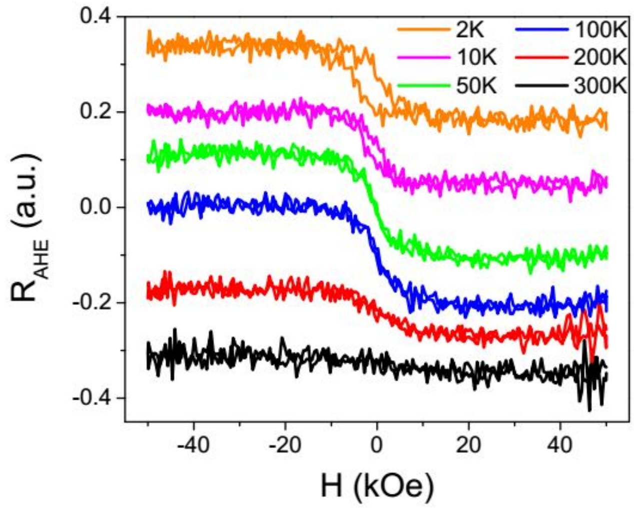

Figure S5. (a) Temperature dependent in-plane magnetic hysteresis loops of a ZrO_2/LAO thin film prepared by oxidizing a ~5 nm sputter-deposited Zr metal at 13 Pa-oxygen environment at 400 ^{o}C. (b) Extracted coercive fields from (a) against measuring temperatures from 10 K to 400 K.

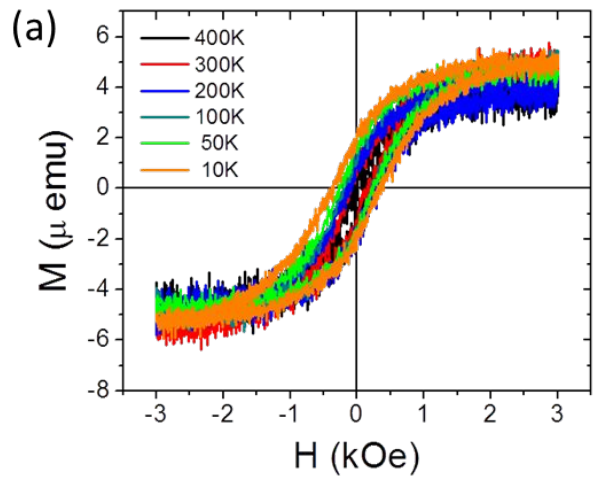

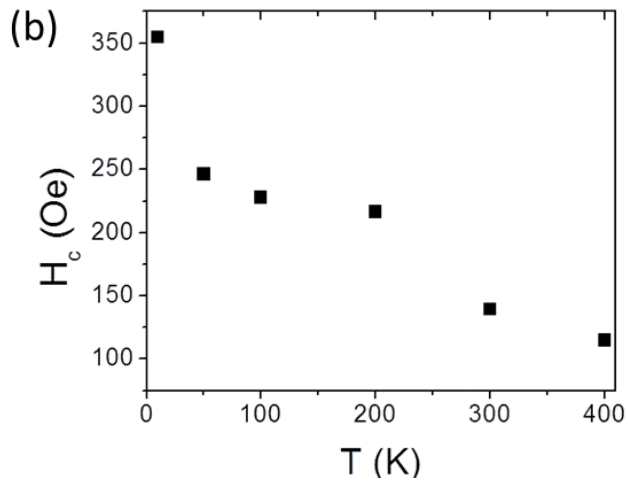

Figure S6. (a) Room temperature and (b) low temperature in-plane MH loops of 30nm-YIG and ~9nm-$ZrTe_2$/~10nm-ZrO_2/YIG. MH loops were measured before and after the deposition of $ZrTe_2$ for the same piece of YIG (Hall bar structure for the heterostructure sample).

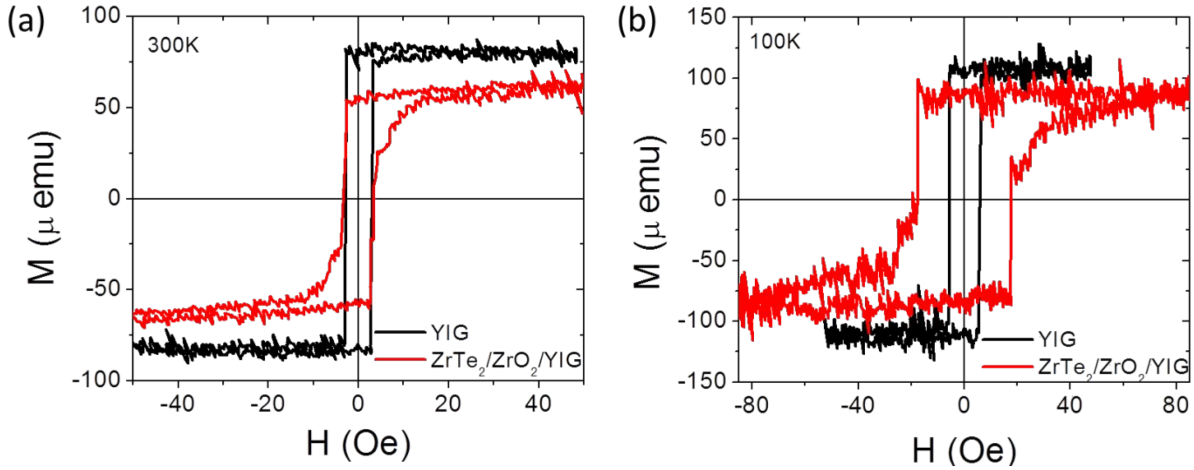

Figure S7: (a) TEM image of $ZrTe_2/ZrO_2$/a-YIG:Te/GGG prepared by depositing $ZrTe_2$ on 10 nm-YIG film, without constructing a Hall bar structure to ensure that the whole YIG layer will form a-YIG:Te so the magnetic signal recorded will exclude that from YIG. It clearly shows the formation of ZrO_2 and complete conversion of YIG to a-YIG:Te layers. (b) AHE of $ZrTe_2$ (30 nm)/ZrO_2 /a-YIG:Te /GGG at 300 K and 2 K. The 300 K data is noisy due to the weaker change of anomalous Hall resistance. (c) Room temperature in-plane normalized MH loops of $ZrTe_2/ZrO_2$/a-YIG:Te/YAG, YIG /YAG and ZrO_2/LAO.

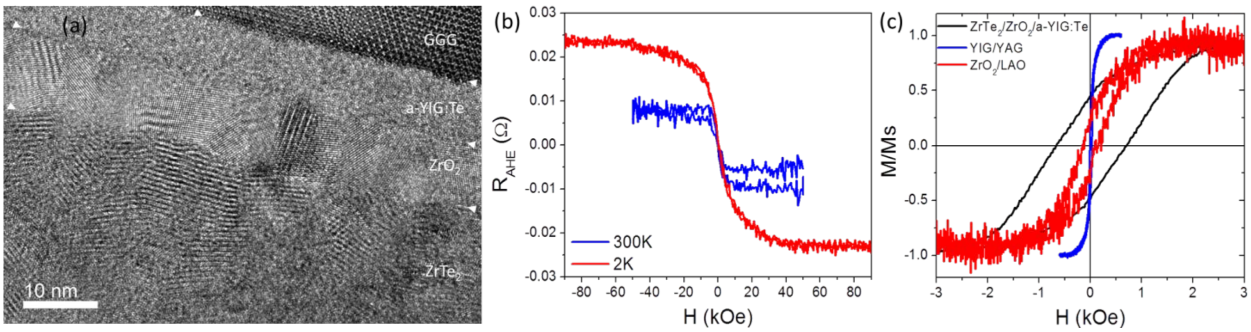

Supplementary Note 1: Electrical contribution from $ZrTe_2$ only

As shown in Figure 3 in our main text, the sheet resistance of $ZrTe_2$ (9 nm)/ZrO_2 (10 nm)/a-YIG:Te (10nm)/YIG at 300 K is ~5×10^3 Ω, which is comparable to that of the 10 nm thick $ZrTe_2$ on SiO_2/Si (~10^3 Ω). The similarity of the resistivity of the heterostructure to $ZrTe_2$ control sample fabricated on SiO_2 indicates that transport in the heterostructure occurs primarily in the $ZrTe_2$ layer. To further confirm the deduction, we have performed control experiments to investigate the underneath ZrO_2/a-YIG:Te/YIG structure. With a very short deposition time (60s) of the Zr-Te target on the YIG/GGG substrate, it was found that ~3 nm ZrO_2 and ~4 nm a-YIG:Te were formed and yet layered $ZrTe_2$ was not (see Figure S2 for TEM image). The resulting ZrO_2 (3 nm)/a-YIG:Te (4 nm)/YIG structure shows quite high resistance at 300 K (> 20 MΩ, which is out of the measuring range of PPMS by Resistivity module) indicating the insulating characteristic. In contrast, the $ZrTe_2$ (4 nm)/ZrO_2 (5 nm)/a-YIG:Te (5 nm)/YIG heterostructure at 300 K shows a much lower resistance (~10^4 Ω). Thus, the AHE recorded in $ZrTe_2$/ZrO_2/a-YIG:Te/YIG is solely electrical contribution from $ZrTe_2$ but not ZrO_2 or a-YIG:Te.

Supplementary Note 2: ZrO_2 as a ferromagnetic with high temperature T_c

We have mimic the formed ZrO_2 by using sputter-deposition of ~5 nm Zr metal films on non-ferromagnetic $LaAlO_3$ substrates at room temperature and subjecting them to annealing at 400 °C in 13 Pa-O_2 environment (which is the O_2 environment for YIG deposition) followed by low O_2 content environment to introduce O_2-vacancies. The films change from conducting to insulating after annealing in O_2, suggesting the formation of oxide layer. The resulting film subjects to VSM measurement and it shows clear MH loops from 10 K to 400 K (Figure S5), suggesting the T_c of ZrO_2 is at least higher than 400 K.

Supplementary Note 3: Magnetic proximity effect in the heterostructure

Since the $ZrTe_2$ film is adjacent to the ZrO_2 layer, we believe that ZrO_2 plays a crucial role for the observed AHE. However, we also notice the difference in saturation field of ZrO_2 and that induced in $ZrTe_2$. It is believed that the interface modulation on the ferromagnetic order can be the possible origin. We have tried to further elucidate the issue by experiments. $ZrTe_2$ was prepared by depositing $ZrTe_2$ on thinner YIG film (10 nm) on GGG and YAG ($Y_3Al_5O_{12}$), aiming to fully amorphourize the YIG layer. TEM examination confirmed the complete conversion of crystalline YIG to a-YIG:Te (see Figure S7(a)), and only ZrO_2 (~8 nm) and a-YIG:Te (~8 nm) formed underneath the layered $ZrTe_2$. The sample on YAG was prepared for VSM measurement since the GGG substrate always shows a large paramagnetic background hindering the characterization of the ferromagnetic feature of the system. As shown in Figure S7(c), the room temperature MH loop of $ZrTe_2$/ZrO_2/a-YIG:Te/YAG shows an enhanced coercive field and saturated magnetization, comparing with the those of YIG/YAG and ZrO_2/LAO. This may support the modulation effect between the different ferromagnetic layers. The electrical transport measurements on the $ZrTe_2$/ZrO_2/a-YIG:Te/GGG sample also reveal obvious AHE behavior (see Figure S7(b)). The results suggest that the imperfect interface may not completely forbid the magnetic proximity effect in this particular case. It is also noticed that the AHE signal shows differences with the magnetization of the heterostructure. This is because AHE is studying the interfacial magnetism of the $ZrTe_2$ layer while VSM shows the magnetization from all of the layers (ZrO_2, a-YIG:Te and YIG).

In summary, we believe that the $ZrTe_2$ layer is actually under influence of all the magnetic layers in different extent in the $ZrTe_2$/ZrO_2/a-YIG:Te/YIG structure. AHE observed in $ZrTe_2$ due to magnetic proximity effect could come from the directly contacted ZrO_2 layer and the ZrO_2 layer may in turn couple with a-YIG:Te and YIG. It is impressive that significant high temperature AHE was realized in such a complex interface. We expect more related studies in this direction to shed light on the issue, which may provide new insight into designing approach to introduce magnetism in TMDs at high temperatures for device applications.